

A stable quasi-solid-state dye-sensitized solar cell with an amphiphilic ruthenium sensitizer and polymer gel electrolyte

PENG WANG¹, SHAIK M. ZAKEERUDDIN*¹, JACQUES E. MOSER¹, MOHAMMAD K. NAZEERUDDIN¹, TAKASHI SEKIGUCHI² AND MICHAEL GRÄTZEL*¹

¹Laboratory for Photonics and Interfaces, Swiss Federal Institute of Technology, CH-1015 Lausanne, Switzerland

²Hitachi Maxell, 1-1-88, Ushitora, Ibaraki-Shi, Osaka 567-8567, Japan

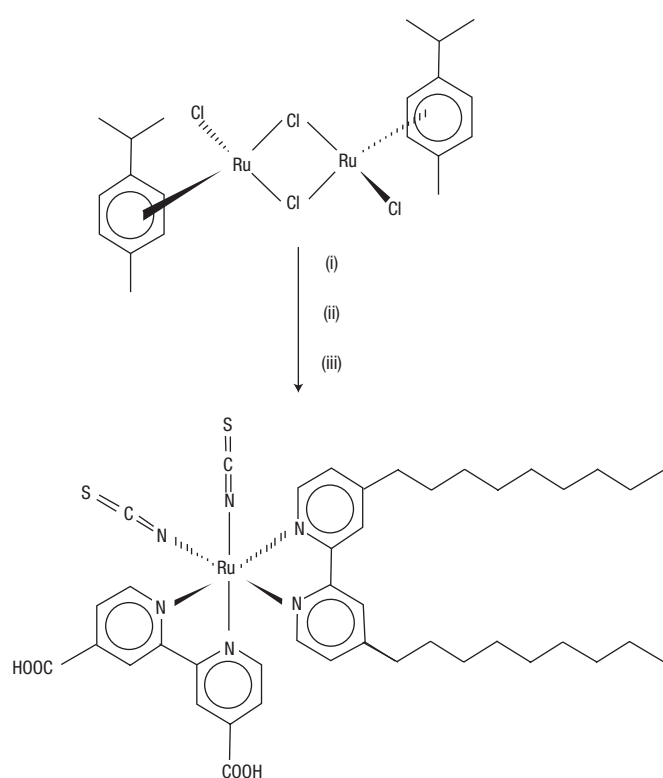
*e-mail: shaik.zakeer@epfl.ch; michael.gratzel@epfl.ch

Published online: 18 May 2003; doi:10.1038/nmat904

Dye-sensitized nanocrystalline solar cells (DSC) have received considerable attention as a cost-effective alternative to conventional solar cells. One of the main factors that has hampered widespread practical use of DSC is the poor thermostability encountered so far with these devices. Here we show a DSC with unprecedented stable performance under both thermal stress and soaking with light, matching the durability criteria applied to silicon solar cells for outdoor applications. The cell uses the amphiphilic ruthenium sensitizer *cis*-RuLL'(SCN)₂ (L = 4,4'-dicarboxylic acid-2,2'-bipyridine, L' = 4,4'-dinonyl-2,2'-bipyridine) in conjunction with a quasi-solid-state polymer gel electrolyte, reaching an efficiency of >6% in full sunlight (air mass 1.5, 100 mW cm⁻²). A convenient and versatile new route is reported for the synthesis of the heteroleptic ruthenium complex, which plays a key role in achieving the high-temperature stability. Ultramicroelectrode voltammetric measurements show that the triiodide/iodide couple can perform charge transport freely in the polymer gel. The cell sustained heating for 1,000 h at 80 °C, maintaining 94% of its initial performance. The device also showed excellent stability under light soaking at 55 °C for 1,000 h in a solar simulator (100 mW cm⁻²) equipped with a ultraviolet filter. The present findings should foster widespread practical application of dye-sensitized solar cells.

Dye-sensitized nanocrystalline solar cells (DSC) provide an economically credible alternative to conventional inorganic photovoltaic devices. Owing to their high-energy conversion efficiency and low production cost, they have received considerable attention over the past decade¹⁻⁴. The mesoscopic texture of the TiO₂ film in these cells significantly increases the cross-section of light harvesting by surface-anchored charge-transfer sensitizers, while maintaining a good contact with electrolytes. In these photovoltaic devices, ultrafast electron injection from a photoexcited dye into the conduction band of an oxide semiconductor, and subsequently dye regeneration and hole transportation to the counter electrode, are responsible for the efficient generation of electricity. Although a respectable 10.4% light-to-electricity conversion efficiency at air mass (AM) 1.5 solar irradiance has been obtained for photovoltaic devices with a panchromatic dye and a liquid electrolyte containing the triiodide/iodide couple⁵, the achievement of long-term stability at temperatures of about 80–85 °C, which is an important requirement for outdoor application of the DSC, still remains a major challenge¹⁻¹¹.

The leakage of liquid electrolyte from such modules, possible desorption of loosely attached dyes, and photodegradation in the desorbed state as well as corrosion of the Pt counter electrode by the triiodide/iodide couple have been suggested as some of the critical factors limiting the long-term performance of the DSC, especially at elevated temperature. Thus considerable efforts have been made to realize devices with high efficiencies that meet the stability criteria for outdoor use. In this context, new counter-electrode materials¹²⁻¹⁴, alternative redox couples¹⁵⁻¹⁷ and sensitizers¹⁸⁻²⁵ have been screened. Additionally, p-type semiconductor^{26,27}, hole conductor²⁸ and polymeric or gel materials incorporating triiodide/iodide as a redox couple²⁹⁻³³ were introduced to substitute the liquid electrolytes by solid-state or quasi-solid-state materials. Numerous investigations of polymer gel electrolytes have been carried out with special emphasis on applications to lithium batteries³⁴. Gelation of the liquid electrolytes mitigate the potential instability against solvent leakage under thermal stress. In this paper, a photochemically stable fluorine polymer, poly(vinylidene fluoride-*co*-hexafluoropropylene (PVDF-HFP), was used to solidify a 3-methoxypropionitrile (MPN)-based liquid electrolyte to obtain a quasi-solid-state gel electrolyte. When used in combination with a new amphiphilic polypyridyl ruthenium dye, this new embodiment of a DSC, which reaches a conversion efficiency under full sunlight of over 6%, shows strikingly high stabilities under both thermal stress at 80 °C and prolonged soaking with light.



Scheme 1 One-pot synthetic route for Z-907 dye.

- (i) DMF, dnbpy, 70 °C, N₂, 4 h.
 (ii) H₂dcbpy, 150 °C, N₂, 4 h.
 (iii) NH₄NCS, 150 °C, N₂, 4 h.

We have previously prepared a series of hydrophobic ruthenium polypyridyl sensitizers for low-power photoelectrochemical cells to increase their tolerance to water in the electrolytes³⁵. The amphiphilic dye Z-907 (*cis*-Ru(H₂dcbpy)(dnbpy)(NCS)₂, where the ligand H₂dcbpy is 4,4'-dicarboxylic acid-2, 2'-bipyridine and dnbpy is 4,4'-dinonyl-2, 2'-bipyridine) was synthesized according to Scheme 1. A novel synthetic route starting from the RuCl₂(*p*-cymene)₂ complex, and using sequential addition of ligands to it at different time intervals, was designed for the synthesis of heteroleptic polypyridyl ruthenium complexes. This method is more facile and gives better yields than that previously reported³⁵.

The conductivity (σ) of the electrolyte used in this study was first examined. This provides information on the mobility of the ions, their interaction with the solvent and on ion-pairing phenomena, which are expected to affect the photovoltaic performance and in particular the fill factor of the solar cell. It is given by³⁶:

$$\sigma(T) = \sum_i |Z_i| F c_i \mu_i = \sum_i \frac{|Z_i|^2 F c_i e D_i}{K_B T} \quad (1)$$

where Z_i , c_i , μ_i and D_i are the charge, concentration, mobility and diffusion coefficient of the i th ion, e is the electronic charge, T is the absolute temperature and K_B and F are the Boltzmann and Faraday constants, respectively. As is apparent from the inset of Fig. 1, the Arrhenius equation³⁶ cannot be used to describe the conductivity–temperature behaviour of the liquid and polymer gel

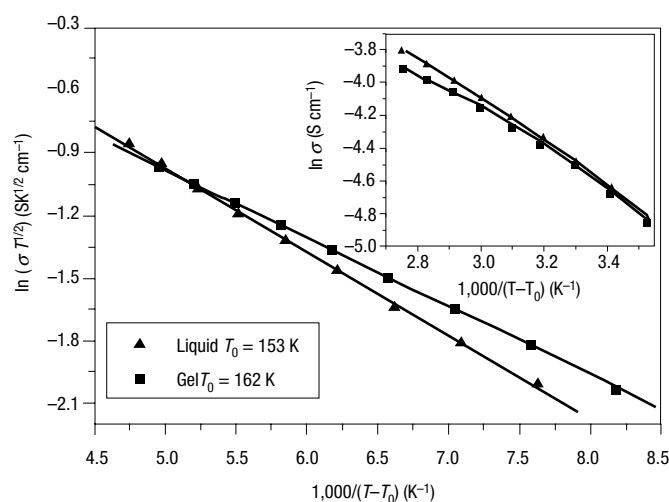


Figure 1 Plots of conductivity–temperature data in the VTF coordinates for the liquid and polymer gel electrolytes. Inset: Arrhenius plots of conductivity–temperature data. σ = specific conductivity; T = absolute temperature; T_0 = glass-transition temperature.

electrolytes. A better fit to the data in Fig. 1 is obtained by the Vogel–Tammann–Fulcher (VTF) equation³⁷.

$$\sigma(T) = AT^{-1/2} \exp[-B/(T-T_0)] \quad (2)$$

In equation (2), A and B are constants and T_0 is the glass-transition temperature. Surprisingly, whereas gelation resulted in a slight decrease in conductivities, for example, from 10.4 to 10.2 mS cm⁻¹ at room temperature, the steady-state voltammograms (Fig. 2) for a Pt ultramicroelectrode in the liquid and polymer gel electrolytes are practically identical. Thus, the triiodide/iodide redox couple can diffuse freely in the liquid domains entrapped by the three-dimensional network of the PVDF-HFP, despite the solid nature of the electrolyte. The apparent diffusion coefficients (D_{app}) of iodide and triiodide can be calculated from anodic and cathodic steady-state currents (I_{ss}) according to the following equation³⁸.

$$I_{ss} = 4ncaFD_{app} \quad (3)$$

where n is the electron number per molecule, a is the microelectrode radius, F is the Faraday constant and c is the bulk concentration of electroactive species. The calculated diffusion coefficients of triiodide and iodide are 3.60×10^{-6} and 4.49×10^{-6} cm² s⁻¹, respectively. Furthermore, using equation (1) the diffusion coefficient of 1,2-dimethyl-propylimidazolium (DMPI) cations in the liquid and polymer gel electrolyte was derived to be 2.39×10^{-7} and

Table 1 Device efficiencies of cells with the liquid and polymer gel electrolytes.

	η (%) at different incident light intensities*			
	0.01 Sun	0.1 Sun	0.5 Sun	1.0 Sun
Liquid	7.5	7.4	6.9	6.2
Gel	7.6	7.3	6.8	6.1

*The spectral distribution of the lamp mimics air mass 1.5 solar light. 1.0 Sun corresponds to an intensity of 100 mW cm⁻².

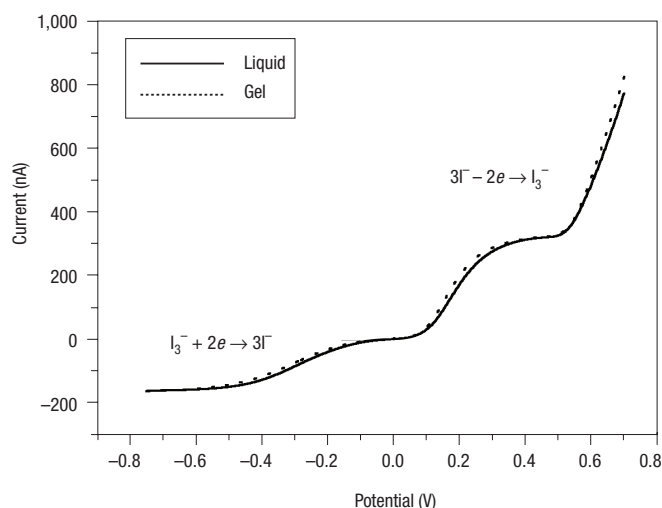


Figure 2 Steady-state voltammograms of the liquid and polymer gel electrolytes with a Pt ultramicroelectrode. Scan rate: 10 mV s⁻¹.

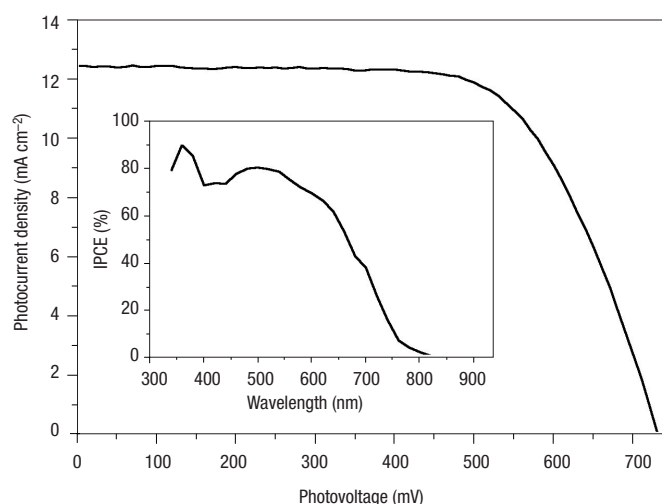


Figure 3 Typical photocurrent density–voltage characteristic of photovoltaic cells. The polymer gel electrolyte and Z-907 dye were at an irradiance of AM 1.5 sunlight (99.8 mW cm⁻²). Cell area: 0.152 cm². The inset is the incident photon-to-current efficiency (IPCE) for the quasi-solid-state cells.

1.55×10^{-7} cm² s⁻¹. The lower value obtained in the gel indicates hydrogen-bonding interaction between DMPI cations and PVDF-HFP copolymer.

Figure 3 shows a typical photocurrent density–voltage curve for cells based on the Z-907 dye and the polymer gel electrolyte under AM 1.5 sunlight illumination. The short-circuit photocurrent density (J_{sc}), open-circuit voltage (V_{oc}), and fill factor (FF) are 12.5 mA cm⁻², 730 mV and 0.67, respectively, yielding an overall energy conversion efficiency (η) of 6.1%. The action spectrum of the photocurrent is shown in the inset of Fig. 3. The incident photon-to-current conversion efficiency (IPCE) reaches a maximum efficiency of 80% at 540 nm. The photovoltaic performance obtained with liquid and polymer gel electrolytes is almost identical (Table 1), indicating that gelation has no adverse effect on the conversion efficiency.

The use of the amphiphilic Z-907 dye in conjunction with the polymer gel electrolyte was found to result in remarkably stable device performance both under thermal stress and soaking with light. The high conversion efficiency of the cell was sustained even under heating for 1,000 h at 80 °C, maintaining 94% of its initial value after this time period as shown in Fig. 4a. The device using the liquid electrolyte retained only 88% of its initial performance under the same conditions. The difference may arise from a decrease in solvent permeation across the sealant in the case of the polymer gel electrolyte. The polymer gel electrolyte is quasi-solid at room temperature, but becomes a viscous liquid (viscosity: 4.34 mPa s) at 80 °C compared with the blank liquid electrolyte (viscosity: 0.91 mPa s). Tolerance of such a severe thermal stress by a DSC having over 6% efficiency is unprecedented. In the case of N-719 dye, the overall efficiency decreased almost 35% during the first week at 80 °C, which clearly reflects the effect of molecular structure of the sensitizer on the stability of DSC. The difference between N-719 and Z-907 is that one of the 4,4'-dicarboxylic acid-2, 2'-bipyridine is replaced with 4,4'-dinonyl-2, 2'-bipyridine to make the dye more hydrophobic. We believe that desorption of N-719 at high temperature resulted in the poor thermostability of related devices. So far, dye-sensitized solar cells have been plagued by performance degradation at temperatures between 80 and 85 °C. The best result obtained in previous studies¹⁰ was a decline in conversion efficiency from initially 4.5 to 3% when the cell was maintained for 875 h at 85 °C.

Figure 5 presents the detailed behaviour of device parameters during the aging tests performed at 80 °C with the DSC containing polymer gel electrolyte. After the first week of aging, the efficiency was moderately enhanced due to an increase in the J_{sc} and FF values. Then a gradually small decrease in V_{oc} , without much variation in J_{sc} and FF, caused a decrease in the overall efficiency by 6%. This is well within the limit of thermal degradation accepted for silicon solar cells.

The device also showed excellent photostability when submitted to accelerated testing in a solar simulator at 100 mW cm⁻² intensity. After 1,000 h of light-soaking at 55 °C the efficiency had dropped by less than 5% (Fig. 4b) for cells covered with an ultraviolet absorbing polymer film. The efficiency difference for devices tested with and without the polymer film was only 4% at AM 1.5 sunlight, indicating a very small sacrifice in efficiency due to ultraviolet filter.

Detailed studies are currently under way to explore the reasons for the remarkable high-temperature stability of solar cells based on the amphiphilic ruthenium sensitizer and the quasi-solid-state gel electrolyte. Here we report on nanosecond time-resolved laser experiments designed to scrutinize the dynamics of the recombination of the electrons injected in the conduction band of TiO₂ (e_{cb}^-) with the oxidized dye (S^+) and the dye regeneration reaction with iodide. Indeed, kinetic competition between these two interfacial charge-transfer processes controls, to a large extent, the photon-to-current conversion efficiency of the photovoltaic devices. Transient absorbance measurements shown in Fig. 6 monitor directly the concentration of oxidized ruthenium sensitizer following photoinduced electron injection from the dye into the conduction band of the semiconductor film^{16,39}. In the absence of iodide (Fig. 6a, trace 1), the decay of the absorption signal reflects the dynamics of recombination of injected electrons with the oxidized dye (S^+). Because the pulsed laser intensity was kept at a very low level (fluence ≤ 40 mJ cm⁻² per pulse at the sample), less than one e_{cb}^-/S^+ charge-separated pair was produced on the average per TiO₂ nanocrystal. This is comparable to the condition prevailing when the photovoltaic device functions under natural sunlight.

The kinetics of S^+ transient absorbance decay could be fitted by a stretched exponential with a typical half-reaction time ($t_{1/2}$) of the

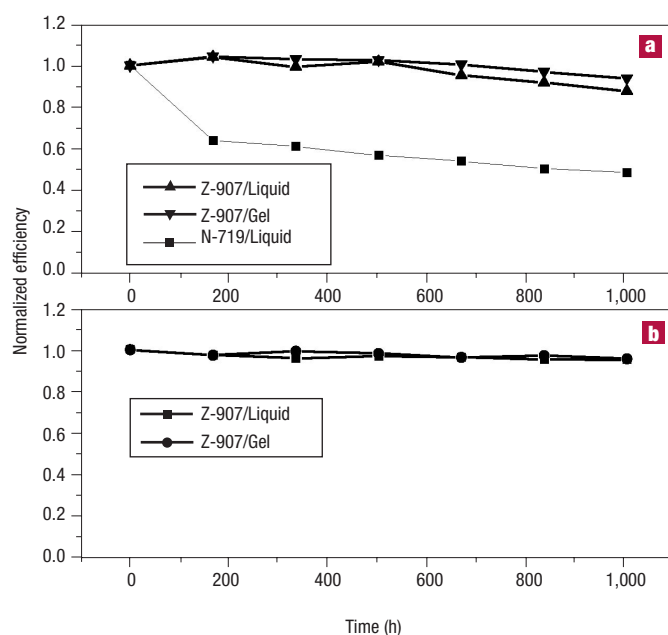


Figure 4 Normalized device efficiencies for cells with the liquid and polymer gel electrolytes. During **a**, accelerated aging at 80 °C and **b**, successive one sun visible-light soaking at 55 °C.

order of 180 μs , similar to what has been reported for the [*cis*-Ru(dcbpy)₂(NCS)₂] dye⁴⁰. Thus the replacement of two carboxylate groups by the hydrocarbon chains does not appear to alter significantly the rate of the interfacial charge recombination process. In the presence of iodide, the decay of the oxidized dye signal is accelerated ($t_{1/2} \approx 30 \mu\text{s}$), showing that the mediator intercepts back-electron transfer. Hardly any difference is observed between the kinetics obtained with the liquid (Fig. 6a, trace 2) and polymer gel (trace 3) electrolytes. In both cases, however, the interception is rather slow compared with what is typically observed for the standard dye N-719 [*cis*-Ru(H₂dcbpy)(dcbpy)(NCS)₂](TBA)₂ under identical conditions³⁹ (Fig. 6b, trace 5, $t_{1/2} \approx 2 \mu\text{s}$). A significant amount of Z-907 cations survives for hundreds of microseconds indicating that the interception is incomplete.

Flash photolysis experiments were conducted under open-circuit conditions, which are in variance with those corresponding to the measurement of IPCE in a short-circuited photovoltaic device. However, the low light intensity used for both laser excitation and probing minimized the build-up of the concentration of conduction-band electrons in TiO₂. In the light of previously reported results⁴⁰, it can be inferred that observed back-electron-transfer kinetics corresponded to a very moderate potential of the nanocrystalline TiO₂ photoanode of $\sim 0 \text{ mV}$ versus Ag/AgCl. The same previous data show that the slow component of the back-transfer kinetics beyond 100 μs is only slightly affected at higher anodic biases. As a consequence, one can estimate that approximately 10–15% of the initial S⁺ species population undergoes recombination with conduction-band electrons. This limits the quantum conversion efficiency and the maximum photocurrent density obtainable in practice. Figure 6b shows the effect of ageing at 80 °C on the kinetics of the interception process. Heat treatment for 72 h clearly produces an increase in the dye regeneration rate, with $t_{1/2}$ diminishing from 30 μs to about 5 μs (Fig. 6b, trace 3). No further change in the interception kinetics is obtained by prolonging the heat exposure of the samples (trace 4). The enhancement of the interception

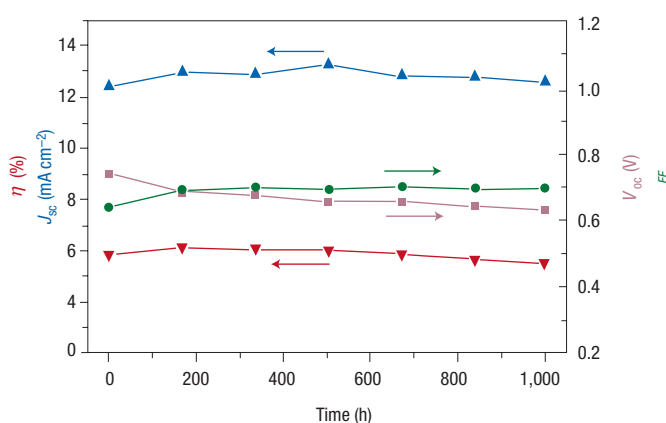


Figure 5 Detail of device parameter variations for cells with polymer gel electrolyte during accelerated aging at 80 °C. η : energy conversion efficiency; J_{sc} : short-circuit photocurrent density; V_{oc} : open current voltage; FF: fill factor.

reaction rate by a factor of six after the heat treatment easily accounts for the increase in overall conversion efficiency after one week of ageing at 80 °C: the photocurrent increases as more charge carriers escape from recombination. This effect is likely to be due to improved self-assembly of the Z-907 dye molecules on the surface of TiO₂ nanocrystals during annealing, and/or electrolyte penetration into cavities containing adsorbed sensitizer molecules where the electrolyte was originally not able to access.

Signals recorded at a probe wavelength of 630 nm are known to be quite sensitive to chemical degradation of Ru^{II}L₂(NCS)₂ dyes. This region of the transient spectrum between 610 and 900 nm is indeed dominated by a ligand-to-metal charge transfer transition of the NCS ligand to the Ru(III) metal centre of the oxidized dyes. Alterations in the coordination geometry of the complex result in a marked decrease⁴¹ of the transient absorbance above 610 nm. Remarkably, no change of the transient absorbance signal amplitude was observed within experimental errors after ageing cells with the Z-907 dye for one week at 80 °C. This indicates that thermal aging does not affect significantly the chemical integrity of the dye molecules.

In summary, we have demonstrated that PVDF-HFP polymer can gel MPN-based liquid electrolyte without hampering charge transport of the triiodide/iodide couple inside the polymer network. Consequently, there is no difference in the conversion efficiencies of dye-sensitized solar cells with liquid and polymer gel electrolytes even at AM 1.5 sunlight. For the first time, long-term thermostable devices with higher than 6% energy conversion efficiency have been obtained by combining an amphiphilic polypyridyl ruthenium sensitizer with a polymer gel electrolyte. The extraordinary stabilities of the device under both thermal stress and soaking with light match the durability criteria applied to solar cells for outdoor use, rendering these devices viable for practical application.

METHODS

All organic solvents used were of puriss quality from Fluka, Switzerland. MPN (Fluka) was distilled before use. Other compounds used were: dnbp (Aldrich, Switzerland), [RuCl₂(*p*-cymene)]₂ (Aldrich), N-methylbenzimidazole (NMBI) (Aldrich), NH₄NCS (Fluka), Sephadex LH-20 (Pharmacia, Sweden), poly(vinylidene fluoride-co-hexafluoropropylene) (PVDF-HFP; Solvay, Belgium), 1,2-Dimethyl-3-propylimidazolium iodide (DMPII) was synthesized according to the method described in our previous work⁴².

ONE-POT SYNTHESIS OF Z-907

In a typical one-pot synthesis of Z-907, [RuCl₂(*p*-cymene)]₂ (0.1 g, 0.16 mmol) was dissolved in DMF (50 ml) and dnbp (0.133 g, 0.32 mmol) then added. The reaction mixture was heated to 60 °C under

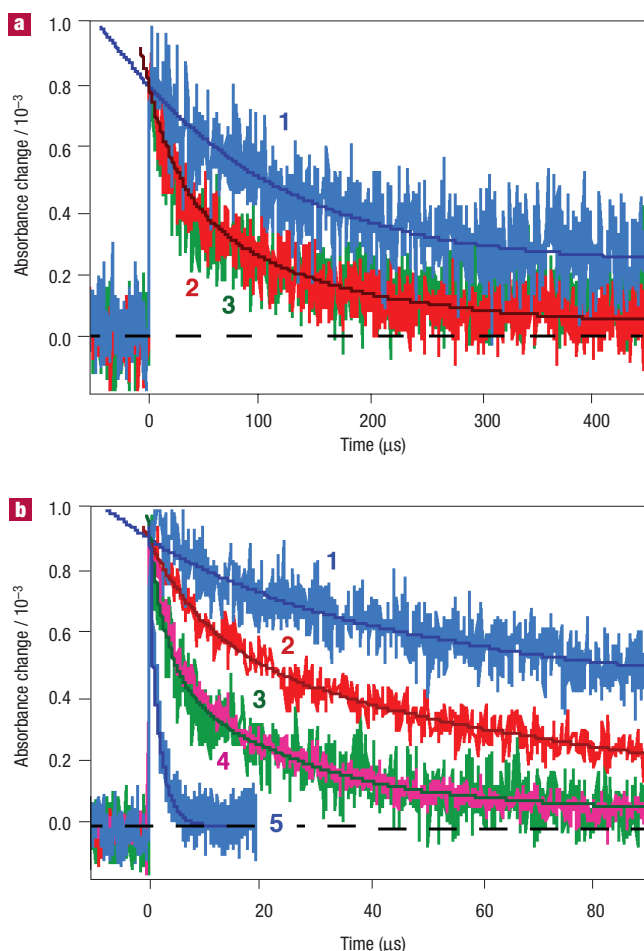


Figure 6 Transient absorbance decay kinetics of the oxidized state of Z-907 dye adsorbed on transparent TiO₂ nanocrystalline films. Measured at 630 nm on pulsed laser excitation at 510 nm (5 ns full-width at half-maximum pulse duration, 40 μJ cm⁻² pulse fluence). **a**, In the presence of pure solvent 3-methoxypropionitrile (1), the liquid electrolyte (2), and the polymer gel electrolyte (3). **b**, Cells containing pure 3-methoxypropionitrile (1), the liquid electrolyte before heat treatment (2), and after keeping at 80 °C for 72 h (3) and 280 h (4), respectively. Trace (5) shows, for direct comparison, the temporal behaviour of the standard N-719 dye under conditions similar to those of trace (2). Solid curves drawn on the top of experimental data are bi-exponential fits of decay kinetics.

nitrogen for 4 h with constant stirring. To this reaction flask H₂dcby (0.08 g, 0.32 mmol) was added and refluxed for 4 h. Finally, excess of NH₄NCS (13 mmol) was added to the reaction mixture and the reflux continued for another 4 h. The reaction mixture was cooled down to room temperature and the solvent was removed by using a rotary evaporator under vacuum. Water was added to the flask and the insoluble solid was collected on a sintered glass crucible by suction filtration. The solid was washed (5 × 20 ml) with pH 12 aqueous solution, distilled water and diethyl ether and dried. On a Sephadex LH-20 column the complex was further purified with methanol as an eluent. ¹H NMR (δ_H/p.p.m. in CD₃OD) 9.72 (d, 1H), 9.28 (d, 1H), 9.08 (s, 1H), 8.92 (s, 1H), 8.55 (s, 1H), 8.42 (s, 1H), 8.28 (d, 1H), 7.88 (d, 1H), 7.70 (t, 2H), 7.40 (d, 1H), 7.05 (d, 1H), 2.95 (t, 2H), 2.75 (t, 2H), 1.95 (m, 2H), 1.40 (m, 26H), 0.90 (t, 6H). Analytical calculation for RuC₂₄H₂₂N₄O₅S₂: C, 57.99; H, 5.98; N, 9.66%. Found: C, 57.90; H, 5.97; N, 9.61%.

FABRICATION OF SOLAR CELLS

A screen-printed double layer of TiO₂ particles was used as the photoanode. A 10-μm-thick film of 20-nm-diameter TiO₂ particles was first printed on the fluorine-doped SnO₂ conducting glass electrode and further coated by 4-μm-thick second layer of 400 nm light-scattering anatase particles (CCIC, Japan). After sintering at 500 °C and cooling down to 80 °C, the TiO₂ electrodes were dye-coated by immersing them into a 0.3 mmol l⁻¹ solution of Z-907 in acetonitrile and *t*-butanol (volume ratio of 1:1) at room temperature for 12 hours and then assembled with thermally planitized conducting glass electrodes. The electrodes were separated by a 35-μm-thick hot-melt ring (Bynel, DuPont) and sealed up by heating. PVDF-HFP (5 wt%) was mixed with the liquid electrolyte consisting of DMPII (0.6 mol l⁻¹),

iodine (0.1 mol l⁻¹), NMBI (0.5 mol l⁻¹) in MPN and heated until no solid was observed. The internal space of the cell was filled with the resulting hot solution using a vacuum pump. After cooling down to room temperature, a uniform motionless polymer gel layer was formed in the cells. The electrolyte-injecting hole made with a sand-ejecting drill on the counter electrode glass substrate was sealed with a Bynel sheet and a thin glass cover by heating. To have a good comparison with the polymer gel electrolyte devices with the liquid electrolyte were also fabricated using the above procedure.

CONDUCTIVITY, VISCOSITY, VOLTAMMETRIC AND PHOTOELECTROCHEMICAL MEASUREMENTS

A CDM210 conductivity meter (Radiometer Analytical, SAS, France) was used to measure conductivities of the liquid and polymer gel electrolytes. The CDC749 conductivity cell (Radiometer Analytical, SAS, France) with a nominal cell constant of 1.70 cm⁻¹ was calibrated with 0.1 mol l⁻¹ KCl aqueous solution before the experiments. Dynamic viscosity measurements were carried out on a microviscosimeter (VT500, Haake, Germany). A DT Hetotherm cycle heat pump (Heto, Denmark) was used to control the temperature of electrolytes. Steady-state voltammograms were recorded on an Autolab P20 electrochemical workstation (Eco Chimie, Netherlands) at 25 °C. A two-electrode electrochemical cell was used, consisting of a Pt ultramicroelectrode with a radius of 5.0 μm as working electrode and a Pt foil as counter electrode. Photoelectrochemical data was obtained with a set-up as explained in our earlier publication⁸.

THERMAL STRESS AND VISIBLE LIGHT-SOAKING TESTS

Hermetically sealed cells were used for long-term stability tests. For thermal stress, the cells were stored in the oven at 80 °C. In light-soaking tests the cells were covered with a 50-μm-thick of polyester film (Preservation Equipment, Norfolk, UK) as an ultraviolet cut-off filter (up to 400 nm) were irradiated at open circuit under a Suntest CPS plus lamp (ATLAS, Netherlands; 100 mW cm⁻², 55 °C).

LASER TRANSIENT ABSORBANCE MEASUREMENTS

Nanosecond pulsed laser excitation was applied using a GWU-355 (GWU-Lasertechnik, Erfstadt-Friesheim, Germany) broadband optical parametric oscillator (OPO) pumped by a Continuum Powerlite 7030 frequency-tripled Q-switched Nd:YAG laser (Continuum, Santa Clara, California, USA). The output of the OPO (30 Hz repetition rate, pulse-width at half-height of 5 ns) was tuned at a wavelength of 510 nm and attenuated by filters. The beam was expanded by a planoconcave lens to irradiate a large cross-section of the sample, whose surface was kept at a 30° angle to the excitation beam. The laser fluence on the sample was kept at a very low level (≤40 μJ cm⁻² per pulse) to ensure that, on average, less than one electron is injected per nanocrystalline TiO₂ particle on pulsed irradiation. The probe light, produced by a continuous wave xenon arc lamp, was passed through a first monochromator tuned at 630 nm, various optical elements, the sample, and a second monochromator, before being detected by a fast photomultiplier tube. Data waves were recorded on a DSA 602A digital signal analyser (Tektronix, Beaverton, Oregon, USA) Satisfactory signal-to-noise ratios were typically obtained by averaging over 3,000 laser shots. Except for normal glass and 8 μm transparent TiO₂ film, sealed cells were used for laser transient absorbance experiments.

Received 24 February 2003; accepted 25 March 2003; published 18 May 2003.

References

- O'Regan, B. & Grätzel, M. A low cost, high efficiency solar cell based on dye-sensitized colloidal TiO₂ films. *Nature* **353**, 737–740 (1991).
- Nazeeruddin, M. K. *et al.* Conversion of light to electricity by *cis*-X₂-bis(2,2'-bipyridyl)-4,4'-dicarboxylate)ruthenium(II) charge transfer sensitizers (X=Cl⁻, Br⁻, I⁻, CN⁻, and SCN⁻) on nanocrystalline TiO₂ electrodes. *J. Am. Chem. Soc.* **115**, 6382–6390 (1993).
- Hagfeldt, A. & Grätzel, M. Molecular photovoltaics. *Accounts Chem. Res.* **33**, 269–277 (2000).
- Grätzel, M. Photoelectrochemical cells. *Nature* **414**, 338–344 (2001).
- Nazeeruddin, M. K. *et al.* Engineering of efficient panchromatic sensitizers for nanocrystalline TiO₂-based solar cells. *J. Am. Chem. Soc.* **123**, 1613–1624 (2001).
- Papageorgiou, N. *et al.* The performance and stability of ambient temperature molten salts for solar cell applications. *J. Electrochem. Soc.* **143**, 3009–3108 (1996).
- Kohle, O. *et al.* The photovoltaic stability of bis(isothiocyanato)ruthenium(II)-bis-2,2'-bipyridine-4,4'-dicarboxylic acid and related sensitizers. *Adv. Mater.* **9**, 904–906 (1997).
- Pettersson, H. & Gruszecski, T. Long-term stability of low-power dye-sensitized solar cells prepared by industrial methods. *Solar Energy Mater. Solar Cells* **70**, 203–211 (2001).
- Kern, R. *et al.* Long-term stability of dye-sensitized solar cells for large area power applications. *Opto-Electron. Rev.* **8**, 284–288 (2001).
- Hinsch, A. *et al.* Long-term stability of dye-sensitized solar cells. *Prog. Photovoltaics* **9**, 425–438 (2001).
- Pettersson, H. *et al.* Manufacturing method for monolithic dye-sensitized solar cells permitting long-term stable low-power modules. *Solar Energy Mater. Solar Cells* **77**, 405–413 (2003).
- Kay, A. & Grätzel, M. Low cost photovoltaic modules based on dye sensitized nanocrystalline titanium dioxide and carbon powder. *Solar Energy Mater. Solar Cells* **44**, 99–117 (1996).
- Saito, Y. *et al.* Application of poly(3,4-ethylenedioxythiophene) to counter electrode in dye-sensitized solar cells. *Chem. Lett.* 1060–1061 (2002).
- Suzuki, K. *et al.* Application of carbon nanotubes to counter electrodes of dye-sensitized solar cells. *Chem. Lett.* **32**, 28–29 (2003).
- Oskam, G. *et al.* Pseudohalogen for dye-sensitized TiO₂ photoelectrochemical cells. *J. Phys. Chem. B* **105**, 6867–6873 (2001).
- Nusbaumer, H. *et al.* Co^{II}(dbbip)₂²⁺ complex rivals tri-iodide/iodide redox mediator in dye-sensitized photovoltaic cells. *J. Phys. Chem. B* **105**, 10461–10464 (2001).
- Sapp, S. A. *et al.* Substituted polypyridine complexes of cobalt(III/II) as efficient electron transfer mediators in dye-sensitized solar cells. *J. Am. Chem. Soc.* **124**, 11215–11222 (2002).
- Ferrere, S. & Gregg, B. A. Photosensitization of TiO₂ by [Fe^{II}(2,2'-bipyridine-4,4'-dicarboxylic acid)₂(CN)₂]⁺: band selective electron injection from ultra-short-lived excited states. *J. Am. Chem. Soc.* **120**, 843–844 (1998).
- Hou, Y.-J. *et al.* Influence of the attaching group and substituted position in the photosensitization behavior of ruthenium polypyridyl complexes. *Inorg. Chem.* **38**, 6320–6322 (1999).
- Monat, J. E. & McCusker, J. K. Femtosecond excited dynamics of an iron(II) polypyridyl solar cell sensitizer model. *J. Am. Chem. Soc.* **122**, 4092–4097 (2000).
- Sauvé, G. *et al.* Dye sensitization of nanocrystalline titanium dioxide with osmium and ruthenium polypyridyl complexes. *J. Phys. Chem. B* **104**, 6821–6836 (2000).

22. Yanagida, M. *et al.* Dye-sensitized solar cells based on nanocrystalline TiO₂ sensitized with a novel pyridylquinoline ruthenium(II) complex. *New J. Chem.* **26**, 963–965 (2002).
23. Li, X. *et al.* New peripherally-substituted naphthalocyanines: synthesis, characterization and evaluation in dye-sensitized photoelectrochemical solar cells. *New J. Chem.* **26**, 1076–1080 (2002).
24. He, J. *et al.* Modified phthalocyanines for efficient near-IR sensitisation of nanostructured TiO₂ electrode. *J. Am. Chem. Soc.* **124**, 4922–4932 (2002).
25. Hara, K. *et al.* Novel polyene dyes for highly efficient dye-sensitized solar cells. *Chem. Commun.* 252–253 (2003).
26. Kumara, G. R. A. *et al.* Fabrication of dye-sensitized solar cells using triethylamine hydrothiocyanate as a CuI crystal growth inhibitor. *Langmuir* **18**, 10493–10495 (2002).
27. O'Regan, B. *et al.* A solid-state dye-sensitized solar cell fabricated with pressure-treated P25-TiO₂ and CuSCN: analysis of pore filling and IV characteristics. *Chem. Mater.* **14**, 5023–5029 (2002).
28. Krüger, J. *et al.* Improvement of the photovoltaic performance of solid-state dye-sensitized device by silver complexation of the sensitizer *cis*-bis(4,4'-dicarboxy-2,2'-bipyridine)-bis(isothiocyanato) ruthenium(II). *Appl. Phys. Lett.* **81**, 367–369 (2002).
29. Cao F., Oskam, G. & Seanson, P. C. A solid-state, dye-sensitized photoelectrochemical cell. *J. Phys. Chem.* **99**, 17071–17073 (1995).
30. Nogueira, A. F., Durrant, J. R. & De Paoli, M. A. Dye-sensitized nanocrystalline solar cells employing a polymer electrolyte. *Adv. Mater.* **13**, 826–830 (2001).
31. Kubo, W. *et al.* Quasi-solid-state dye-sensitized solar cells using room temperature molten salts and a low molecular weight gelator. *Chem. Commun.* 374–375 (2002).
32. Wang, P. *et al.* High efficiency dye-sensitized nanocrystalline solar cells based on ionic liquid polymer gel electrolyte. *Chem. Commun.* 2972–2973 (2002).
33. Wang, P. *et al.* Gelation of ionic liquid-based electrolytes with silica nanoparticles for quasi-solid-state dye-sensitized solar cells. *J. Am. Chem. Soc.* **125**, 1166–1167 (2003).
34. Tarascon, J.-M. & Armand, M. Issues and challenges facing rechargeable lithium batteries. *Nature* **414**, 359–367 (2001).
35. Zakeeruddin, S. M. *et al.* Design, synthesis, and application of amphiphilic ruthenium polypyridyl photosensitizers in solar cells based on nanocrystalline TiO₂ films. *Langmuir* **18**, 952–954 (2002).
36. Kataoka, H. *et al.* Interactive effect of the polymer on carrier migration nature in the chemically cross-linked polymer gel electrolyte composed of poly(ethylene glycol) dimethacrylate. *J. Phys. Chem. B* **106**, 12084–12087 (2002).
37. Gu, G. Y. *et al.* 2-Methoxyethyl (methyl) carbonate-based electrolytes for Li-ion batteries. *Electrochim. Acta* **45**, 3127–3139 (2000).
38. Wightman, R. M. & Wipf, D. O. in *Electroanalytical Chemistry* Vol. 15 (ed. Bard, A. J.) 283 (Marcel Dekker, New York, 1989).
39. Pelet, S., Moser, J. E. & Grätzel, M. Cooperative effect of adsorbed cations and iodide on the interception of back electron transfer in the dye sensitization of nanocrystalline TiO₂. *J. Phys. Chem. B* **104**, 1791–1795 (2000).
40. Haque, S. *et al.* Parameters influencing charge recombination kinetics in dye-sensitized nanocrystalline titanium dioxide films. *J. Phys. Chem. B* **104**, 538–547 (2000).
41. Moser, J. E. *et al.* Comment on "Measurement of ultrafast photoinduced electron transfer from chemically anchored Ru-dye molecules into empty electronic states in a colloidal anatase TiO₂ film". *J. Phys. Chem. B* **102**, 3649–3650 (1998).
42. Bonhôte, P. *et al.* Hydrophobic, highly conductive ambient-temperature molten salts. *Inorg. Chem.* **35**, 1168–1178 (1996).

Acknowledgements

We are grateful to P. Péchy, I. Exnar and P. Liska for fruitful discussions, T. Koyanagi (CCIC, Japan) for providing the 400 nm TiO₂ particles and P. Comte for TiO₂ film fabrication. The Swiss Science Foundation, Swiss Federal Office for Energy (OFEN) and the European Office of US Air Force under Contract No. F61775–00–C0003 have supported this work. Correspondence and requests for materials should be addressed to S.M.Z. or M.G.

Competing financial interests

The authors declare that they have no competing financial interests.

ERRATUM

A stable quasi-solid-state dye-sensitized solar cell with an amphiphilic ruthenium sensitizer and polymer gel electrolyte

Peng Wang, Shaik M. Zakeeruddin, Jacques E. Moser, Mohammad K. Nazeeruddin, Takashi Sekiguchi and Michael Grätzel

Nature Materials 2, 402–407 (2003).

In this article, the x axis of the inset in Fig. 1 was incorrectly shown to be $1,000/(T-T_0)$ (K^{-1}), whereas it should be $1,000/T$ (K^{-1}). The corrected version of Fig. 1 appears below.

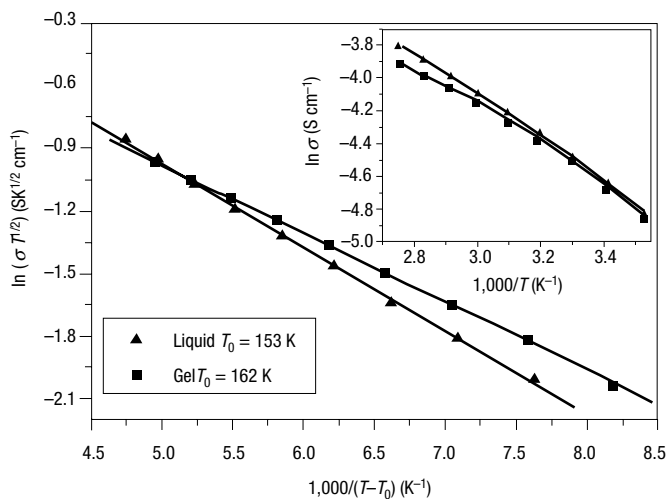


Figure 1 Plots of conductivity–temperature data in the VTF coordinates for the liquid and polymer gel electrolytes. Inset: Arrhenius plots of conductivity–temperature data. σ = specific conductivity; T = absolute temperature; T_0 = glass-transition temperature.